

## PLANES OF SATELLITES, AT ONCE TRANSIENT AND PERSISTENT

TILL SAWALA\* 

Department of Physics, University of Helsinki, Gustaf Hällströmin katu 2, FI-00014 Helsinki, Finland

## Abstract

The appearance of highly anisotropic planes of satellites around the Milky Way and other galaxies was long considered a challenge to the standard cosmological model. Recent simulations have shown such planes to be common, but they have been described as either “transient”, short-lived alignments, or “persistent”, long-lived structures. Here we analyse Milky Way analogue systems in the cosmological simulation TNG-50 to resolve this apparent contradiction. We show that, as the satellite populations of individual hosts rapidly change, the observed anisotropies of their satellite systems are invariably short-lived, with lifetimes of no more than a few hundred million years. However, when the progenitors of the same satellites are traced backwards, we find examples where those identified to form a plane at the present day have retained spatial coherence over several Gyr. The two ostensibly conflicting predictions for the lifetimes of satellite planes can be reconciled as two perspectives on the same phenomenon.

*Subject headings:* cosmology: theory, dark matter – galaxies: Local Group, dwarf – methods: numerical

## 1. INTRODUCTION

Planes of satellites, or more generally, the anisotropic distributions of satellite galaxies around their hosts, have long been considered a challenge to the  $\Lambda$ CDM ( $\Lambda$  Cold Dark Matter) cosmological model (e.g. Kroupa et al. 2005; Kroupa 2012; Bullock & Boylan-Kolchin 2017; Perivolaropoulos & Skara 2021; Pawłowski 2018; Pawłowski & Sohn 2021; Boylan-Kolchin 2021; Sales et al. 2022). In the standard model of hierarchical galaxy and structure formation (Davis et al. 1985), satellite galaxies populate substructures of only mildly triaxial (e.g. Frenk et al. 1988) dark matter halos. While the distributions of satellite galaxies surrounding the Milky Way (hereafter MW, Lynden-Bell 1976), M31 (Ibata et al. 2013), and many other galaxies (e.g. Ibata et al. 2014; Müller et al. 2018), appear to be highly anisotropic, the conjecture that  $\Lambda$ CDM predicts fairly isotropic distributions was largely supported by early numerical studies (e.g. Kroupa et al. 2005; Libeskind et al. 2005; Pawłowski & Kroupa 2020).

More recent, high-resolution simulations have shown that  $\Lambda$ CDM does predict anisotropic satellite systems, provided artificial numerical disruption of satellites near the centre is avoided (e.g. Sawala et al. 2023a; Xu et al. 2023; Santos-Santos et al. 2023; Zhao et al. 2023; Uzeirbegovic et al. 2024). However, the nature of the planes reported by different authors appears incompatible. While some authors have reported that  $\Lambda$ CDM can only produce short-lived satellite systems that dissolve within a few hundred million years (e.g. Buck et al. 2016; Shao et al. 2019; Santos-Santos et al. 2020; Müller et al. 2021; Samuel et al. 2021; Sawala et al. 2023a; Xu et al. 2023), others have found long-lived anisotropies that remain intact for several gigayears (e.g. Santos-Santos et al. 2023; Gámez-Marín et al. 2024, 2025; Madhani et al. 2025).

Furthermore, while Fernando et al. (2017, 2018) have shown that planes of satellites within realistic dark mat-

ter halos are dynamically unstable and must quickly disperse due to torques imparted in non-spherical potentials and by substructures, others have explained how accretion from the cosmic web (e.g. Libeskind et al. 2015; Gámez-Marín et al. 2024) and / or group infall (e.g. Li & Helmi 2008) could lead to the emergence of long-lived anisotropies.

With two ostensibly incompatible results for the nature of satellite planes in  $\Lambda$ CDM now widely discussed, it is unclear what the model actually predicts, and it may even be questioned whether the “plane of satellites problem” is solved at all. In this work, we set out to resolve the apparent inconsistency by showing that, in fact, the same satellite systems can appear either “transient” or “persistent”.

## 2. SATELLITE SYSTEMS IN TNG-50

Previous works have used differing definitions of anisotropy or planarity and have analysed different (sometimes unpublished) simulation data. Notwithstanding the merits of more sophisticated metrics, we will focus here on the most widely used measure of spatial anisotropy,  $c/a$ , where  $c$  and  $a$  are the square roots of the smallest and largest eigenvalues of the unweighted inertia tensor,

$$\mathbf{I}_{ij} = \sum_{k=1}^N x_{k,i} x_{k,j},$$

where  $\mathbf{x}_k$  are the positions of the satellites relative to the host centre. We also limit our presentation to the  $N = 11$  brightest satellites of each system as analogues to the 11 “classical” MW satellites that define its canonical plane, but adopting  $N = [9 \dots 13]$  yields qualitatively similar results.

We consider host and satellite galaxies from the sample of MW analogues described in Pillepich et al. (2024), drawn from the ILLUSTRIS TNG-50 cosmological hydrodynamical simulation (hereafter TNG-50, Nelson et al. 2019a,b; Pillepich et al. 2019). The simulation evolves

\*Email: till.sawala@helsinki.fi

$2160^3$  dark-matter particles with a mass of  $4.5 \times 10^5 M_\odot$  and  $2160^3$  initial gas cells with an average mass of  $8.5 \times 10^4 M_\odot$  in a periodic volume of  $51.7^3 \text{ cMpc}^3$  (comoving Mpc), with details provided in the references above.

Planes of satellites in TNG-50 have already been extensively studied, including by Pawłowski & Sohn (2021), who found a lack of analogues to M31’s satellite plane(s), Seo et al. (2024), who reported a low frequency of analogues to the MW’s plane of satellites, Hu & Tang (2025), who found planar structures in 11% of MW analogues, Xu et al. (2023), who studied in detail a thin but transient plane of satellites around one particular MW analogue, and Gámez-Marín et al. (2025), who report the existence of “kinematically coherent” subsets of satellites for a number of hosts.

In total, the catalogue of Pillepich et al. (2024) contains 198 MW analogues at the present time ( $z = 0$ , lookback time  $t = 0$ ). From these, we select the 190 objects (96%) which are centrals, i.e. the most massive substructures within their respective dark matter halos, so that halo properties such as  $r_{200}$ , the radius of a sphere whose density is  $200 \times$  the mean density, and  $M_{200}$ , the mass enclosed within  $r_{200}$ , can be identified and directly attributed to them.

We use the location of the most bound particle of a subhalo to define its position, and identify as satellite galaxies all subhalos that contain stars, and which are located within  $r_{\text{lim}}(t) = 1.2 \times r_{200}(t)$  from the host. This factor, resulting in a median of  $r_{\text{lim}}(t = 0) = 277 \text{ kpc}$ , corresponds to the canonical definition of  $r_{\text{lim}}(t = 0) = 300 \text{ kpc}$  for studies of MW satellites, whose  $r_{200}$  at  $t = 0$  is estimated to be  $\sim 250 \text{ kpc}$  (choosing  $r_{\text{lim}} = r_{200}$  slightly reduces the sample size and the typical time satellites spend inside  $r_{\text{lim}}$ , but yields very similar results for all metrics we discuss). By this definition, 188 out of 190 systems (99%) have at least 11 satellite galaxies at  $t = 0$ . Where there are more than 11 satellites, we choose the subset with the highest stellar masses.

Additionally, we require that the host and all 11 satellites identified at  $t = 0$  have main-branch progenitors for at least 19 additional outputs (lookback time of 3.27 Gyr, corresponding to a redshift of  $z = 0.28$  and a mean snapshot interval of  $\sim 0.16 \text{ Gyr}$ ), a condition fulfilled by 109 systems (57%), and that at least 11 satellite galaxies are found within  $r_{\text{lim}}(t)$  of the particular host for the same time interval, which 181 systems (95%) satisfy. This choice of lookback time interval represents a compromise: at  $t > 3 \text{ Gyr}$ , we can clearly distinguish “short-lived” and “long-lived” features, while also retaining a large enough sample of systems for which we can trace the progenitors of all  $N = 11$  satellites, given the finite mass resolution of the simulation.

We remove one system whose  $r_{200}$  repeatedly changes by more than 50% between adjacent snapshots in our lookback time interval, indicating a close interaction with a more massive halo and resulting in discontinuities in our satellite definition. None of the remaining systems change in  $r_{200}$  by more than 10% between any two snapshots.

Our final sample contains 101 of the 190 systems (53%) that fulfil all criteria. While our selection could introduce biases (such as preferentially selecting higher-mass systems), the halo mass distribution closely matches the

parent sample ( $M_{200,N=190} = 1.36_{-0.53}^{+1.13} \times 10^{12} M_\odot$  vs.  $M_{200,N=101} = 1.30_{-0.43}^{+1.08} \times 10^{12} M_\odot$ ), and is compatible with mass estimates of  $\sim 10^{12} M_\odot$  for the MW (e.g. Sawala et al. 2023b; Hunt & Vasiliev 2025).

It must be noted that, despite its relatively high mass resolution, TNG-50 likely still suffers from the artificial disruption of satellites (van den Bosch & Ogiya 2018). For comparison, Grand et al. (2021) showed that an even higher mass resolution of  $3 \times 10^5 M_\odot$  is still insufficient to prevent numerical disruption of substructures near the centre. As shown by Sawala et al. (2023a), one consequence of this is a much lower detectable anisotropy, making simulations like TNG-50 unsuitable for quantifying the frequency of satellite planes predicted by the underlying cosmological model. In our case, none of the systems in the sample reaches the MW’s low  $c/a = 0.183$ , and only one matches the MW’s high Gini coefficient of inertia (see Sawala et al. 2023a), an indicator of artificial disruption and artificially reduced anisotropy.

However, we are not concerned with quantifying the incidence of satellite planes, but in their time evolution. For this purpose, we consider systems with  $c/a$  in the lowest quartile ( $c/a < 0.34$ ) at  $t = 0$ . The large sample size, the accessibility of the data, and the extensive prior analysis make TNG-50 ideal for demonstrating a more general principle.

### 3. HOST-CENTRIC AND SATELLITE-CENTRIC FRAMES

We follow the evolution of the satellite systems and their spatial anisotropies in two complementary frames. In the *host-centric* frame, we follow the main progenitor of each MW analogue backwards in time. At each output, we re-select all subhalos within  $r_{\text{lim}}(t)$  of the host’s centre at that time, and measure the properties of the 11 satellites with the greatest stellar mass. In the *satellite-centric* frame, we follow the main progenitors of each of the 11 most massive satellites identified at  $t = 0$  over the same time interval. At each output, we measure  $c/a$  for the same subhalos, irrespective of their positions and their stellar-mass rank at that time.

In the *host-centric* frame, we thus trace the evolution of the anisotropy of the (potentially changing) satellite population surrounding each host. In particular, we may ask how long a given satellite plane found at  $t = 0$  would have been identified surrounding the same galaxy, had its satellite system been examined independently and under the same conditions under which it was examined at  $t = 0$ . Additionally, we track the change in the makeup of the satellite population, and ask for how long the *same* subset of subhalos would have been identified as each host’s 11 brightest satellites.

In the *satellite-centric* frame, we always follow the evolution of a fixed set of subhalos identified to be the 11 most massive satellites of the host at  $t = 0$ , irrespective of whether they were among the 11 brightest satellites or whether they were even within  $r_{\text{lim}}$  at some earlier time. In this way, we may ask for how long the particular subset of subhalos identified as an anisotropic satellite system at  $t = 0$  had maintained its anisotropy.

Both perspectives are identical at  $t = 0$ , but diverge with increasing lookback time, as new satellites have fallen in, and previously existing ones have become disrupted. As we will show, in the *host-centric* frame,

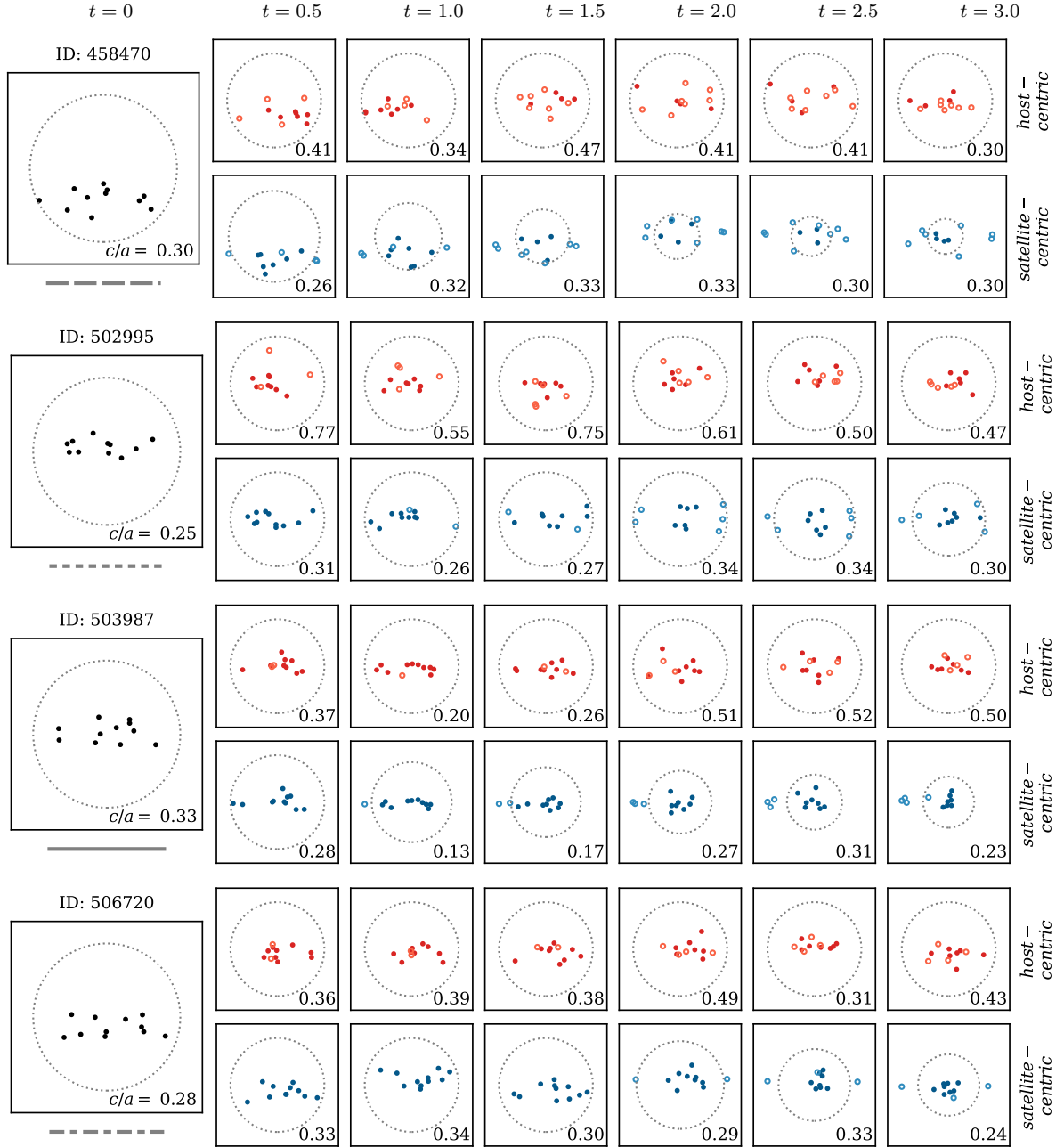


FIG. 1.— Position of the 11 brightest satellites, projected edge-on (i.e. in the plane of the minor and major axes of the inertia tensor), in four example systems, at the present day (left), and six lookback times up to 3 Gyr, in the *host-centric* frame (top, red) and the *satellite-centric* frame (bottom, blue). In the *host-centric* frame, filled circles denote satellites that are part of the  $t = 0$  sample, in the *satellite-centric* frame, filled circles denote subhalos inside  $r_{\text{lim}}(t)$ . On each panel,  $r_{\text{lim}}$  is plotted for scale, and the value of  $c/a$  is given. The ID above the  $t = 0$  panel identifies the host subhalo in the simulation at  $t = 0$ , and the line style below the  $t = 0$  panel identifies the system in Figure 2. In these four systems, the spatial anisotropy varies rapidly in the *host-centric* frame, but remains stable in the *satellite-centric* frame.

any host's satellite plane has been short-lived, while the *satellite-centric* frame reveals several examples of long-lived anisotropies.

#### 4. THE ANISOTROPY EVOLUTION

Figure 1 shows four satellite systems that are anisotropic at  $t = 0$ . For each system, the larger, leftmost panels show the positions of the 11 brightest satellites at  $t = 0$ . The next six rows show the positions at lookback times up to 3 Gyr, in both the *host-centric* frame (upper row, red) and in the *satellite-centric* (lower row, blue) frame. On all panels,  $r_{\text{lim}}(t)$  of the host halo is shown

for scale.

These examples show clear differences. Firstly, in the *host-centric* frame, the identity of the 11 brightest satellites changes quickly: in all four cases, at least two satellites are different at a lookback time of only 0.5 Gyr. This change in the composition of satellite samples is caused by two effects: satellites that are part of the  $t = 0$  sample but which have only recently fallen in, and satellites that were part of the earlier sample, but which have been tidally stripped or destroyed at  $t = 0$ . Both contribute to the rapid evolution of the anisotropy in the *host-centric*

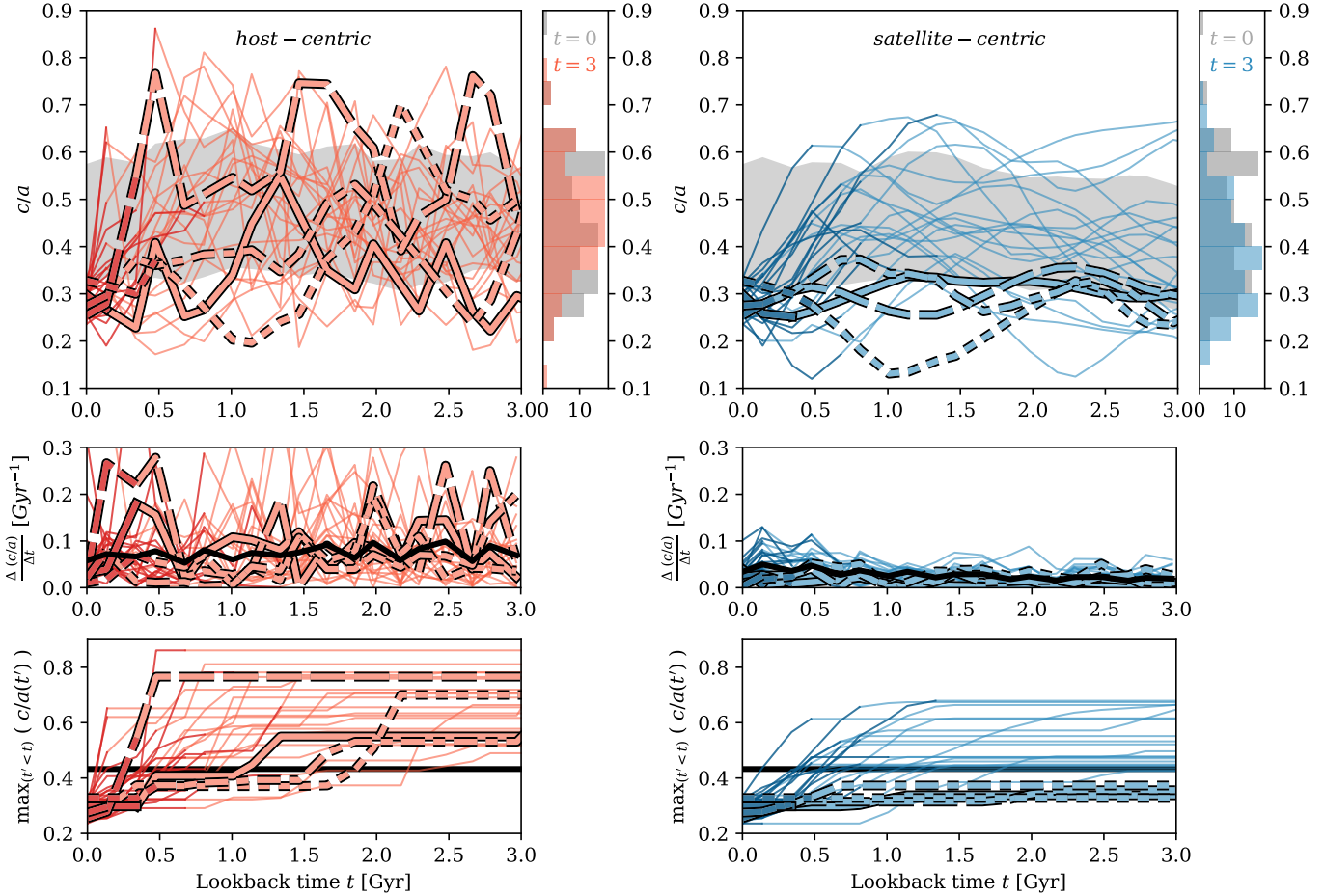


FIG. 2.— Top: evolution of the anisotropy,  $c/a$ , in the *host-centric* frame (left) or *satellite-centric* frame (right). Middle: rate of change of  $c/a$  between individual snapshots. Bottom: maximum value of  $c/a$  up to lookback time  $t$ . Individual lines show the 25 systems in the lowest quartile of  $c/a$  at  $t = 0$ , with the four systems described in Figure 1 highlighted. Dark line segments indicate the interval in which the system contains the same satellites as at  $t = 0$  (*host-centric* frame), or when all satellites are within  $r_{\text{lim}}$  (*satellite-centric* frame). Grey bands on the top panels show  $\pm 1\sigma$ -equivalent percentiles for all 101 systems, with histograms showing the corresponding distributions at  $t = 0$  and  $t = 3$  Gyr. Black lines in the middle and bottom panels show the moving median and the median at  $t = 0$ , respectively. Only in the *satellite-centric* frame do several systems maintain a persistently high anisotropy.

frame.

By contrast, in the *satellite-centric* frame, at earlier times, an increasing fraction of the satellites that define the plane at  $t = 0$  are found outside  $r_{\text{lim}}$ . In particular, at larger lookback times, the progenitors of present-day plane members can be far outside their (future) host's halo. Subhalos outside the halo are not subject to the torques that change their orbits within the halo. The result is a much more gradual evolution of the anisotropy, and the existence of long-lived anisotropies previously reported.

This stark difference in evolution between the two frames can also be observed in larger samples. The top row of Figure 2 shows the evolution of the anisotropy for all systems with  $c/a$  in the lowest quartile ( $c/a < 0.34$ ) at  $t = 0$ . The middle and bottom row show the absolute rate of change in anisotropy between adjacent snapshots,  $\Delta(c/a)/\Delta t$ , and the running maximum of  $c/a$  as a function of lookback time,  $\max_{t' \leq t} (c/a(t'))$ . For panels on the left, the *host-centric* frame is adopted, while those on the right show the *satellite-centric* view. Each line represents an individual system, bold lines identify the four systems shown in Figure 1.

In the *host-centric* frame, for each system, dark line segments denote the time intervals when the satellite sample consists of the same 11 individual satellites identified at  $t = 0$ , while light line segments indicate a change in the satellite composition. In the *satellite-centric* frame, dark segments denote the time intervals when all 11 subhalos are within  $r_{\text{lim}}$ . None of the 25 systems maintain the same 11 brightest satellites for more than 1 Gyr in the *host-centric* frame, and in no case do all the progenitors of the 11 brightest satellites remain within  $r_{\text{lim}}$  for more than 1.5 Gyr.

Starting from the same high anisotropies at  $t = 0$ , most systems show a “regression to the mean” in both the *host-centric* frame and the *satellite-centric* frame, consistent with chance alignments in both frames. However, the anisotropy changes much more rapidly, and more universally, in the *host-centric* frame. Here, even the slowest-changing systems undergo rapid changes in anisotropy, and no system has maintained a value of  $c/a$  below the median value throughout the 3 Gyr time interval. In the *host-centric* frame, all satellite planes would be considered short-lived.

While large (although not as rapid) changes are also

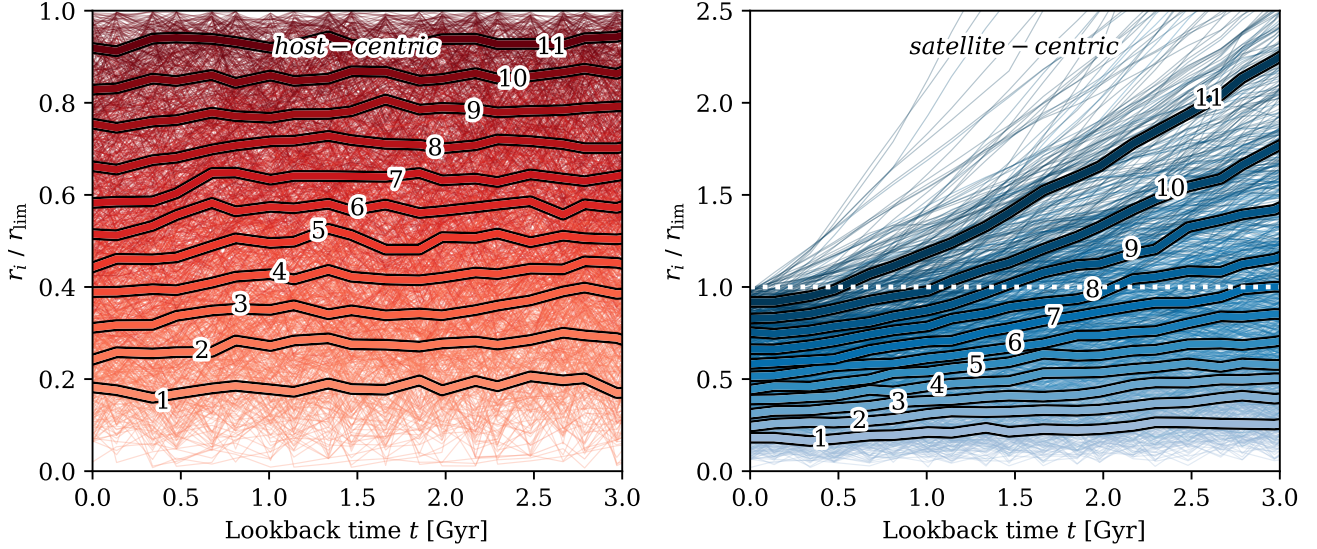


FIG. 3.— Evolution of the distance of the  $i$ th innermost satellite to the centre, normalised by  $r_{\lim}(z)$ , in the *host-centric* frame (left), or *satellite-centric* frame (right). Thick lines show the median ratio, thin lines of corresponding colours show individual systems. In the *host-centric* frame, by definition, all satellites are always inside  $r_{\lim}(t)$ , and normalised by  $r_{\lim}(t)$ , the average radial profile shows little evolution. In the *satellite-centric* frame, the system “expands” with increasing lookback time. Of the 11 satellites at  $t = 0$ , two typically fell in less than one Gyr ago, and four less than two Gyr ago.

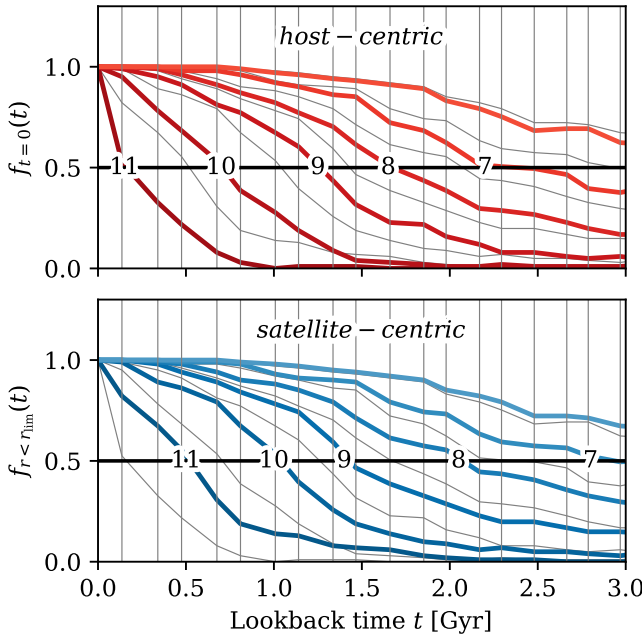


FIG. 4.— Top: Fraction of systems for which at least  $N$  of 11 satellites of the  $t = 0$  system are part of the system in the *host-centric* frame. Bottom: Fraction of systems for which at least  $N$  of 11 satellites are found within  $r_{\lim}$  in the *satellite-centric* frame. Grey lines show the corresponding lines of the other panel, vertical lines indicate the timing of snapshots.

common in the *satellite-centric* frame, several systems, including those highlighted, only undergo a mild change in anisotropy, maintaining close to their present value for several Gyr in lookback time. In the *satellite-centric* frame, several systems have maintained long-lived anisotropies, but these would be detected as “planes of satellites” for only a fraction of the time, as some of the subhalos that constitute the  $t = 0$  plane have only recently been accreted.

The largest difference between the two frames is caused by the late infall of satellites. This results in an increasing fraction of the progenitors of the  $t = 0$  located outside of the halo, and an increasing change of the in-halo satellite population, with increasing lookback time. In the *satellite-centric* frame, the systems effectively expand beyond the host halo with increasing lookback time, maintaining or often increasing their anisotropies. By contrast, in the *host-centric* frame, the subhalo populations are exchanged over time.

In Figure 3, the difference is illustrated by considering the radial distribution of satellites in both the *host-centric* and the *satellite-centric* frame. In the *host-centric* frame, where satellites are identified anew within  $r_{\lim}$  at each snapshot, the average radial distribution does not change, with the innermost of the 11 satellites typically found close to  $0.2 \times r_{\lim}$ , and the outermost typically close to  $0.9 \times r_{\lim}$ . By contrast, in the *satellite-centric* frame, where individual satellites are traced, the systems “expand” with increasing lookback time: one satellite is typically outside  $r_{\lim}$  in under 0.5 Gyr, and by 3 Gyr, nearly half of the subhalos identified at  $t = 0$  had not yet fallen into  $r_{\lim}$ .

Figure 4 shows the fraction of systems, as a function of time, for which the  $N$  satellites are within  $r_{\lim}$  in the *satellite-centric* frame, and the fraction of systems, as a function of time, for which the set of satellites in the *host-centric* frame contains  $N$  of the same satellites as those identified at  $t = 0$ .

As subhalos cross  $r_{\lim}$ , both fractions decrease with increasing lookback time. In the *satellite-centric* frame, the sets of subhalos contain an increasing number of subhalos outside  $r_{\lim}$ . In the *host-centric* frame, these subhalos are replaced by different subhalos within  $r_{\lim}$ . However, for a given  $N$ , the decrease in  $f_{t=0}$  proceeds slightly faster than that in  $f_{r < r_{\lim}}$ . This is because the replacement of subhalos can also be caused by the appearance, at increasing lookback times, of satellites

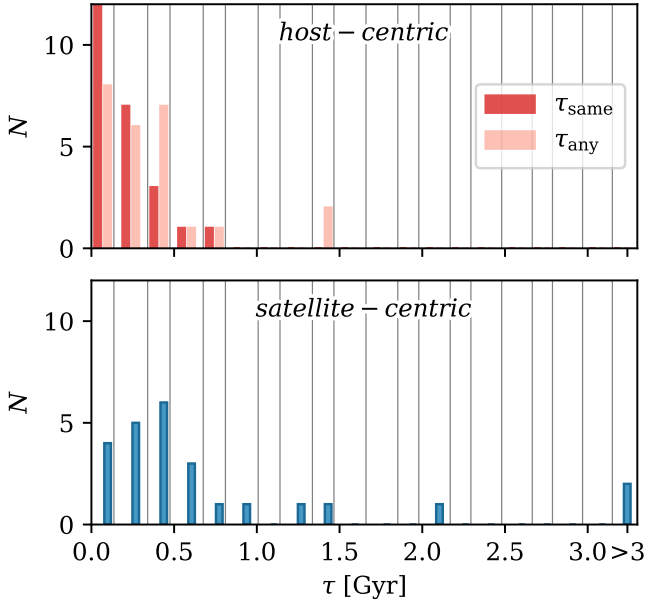


FIG. 5.— Lifetime of satellite planes in the *host-centric* frame (top) and the *satellite-centric* frame (bottom). In the *host-centric* frame, we distinguish between planes that contain the *same* satellites, and *any* satellite plane in the same halo (including those whose membership has changed). Vertical lines indicate the timing of the snapshots.

that were subsequently destroyed (or in rare cases, escaped) by  $t = 0$ .

##### 5. LIFETIMES OF SATELLITE PLANES

In Figure 5, we show the distribution for the lifetime,  $\tau$ , of satellite planes, i.e. of satellite systems in the lowest quartile of  $c/a$  at  $t = 0$ . In the *host-centric* frame, we define  $\tau_{\text{same}}$  as the time for which the *same* set of satellites identified at  $t = 0$  has maintained a value of  $c/a$  in the lowest quartile within  $r_{\text{lim}}$ , and  $\tau_{\text{any}}$  as the time for which the 11 brightest satellites of the system have maintained the same anisotropy, regardless of membership changes over time. In the *satellite-centric* frame,  $\tau$  is the time for which the same set of subhalos has maintained a value in the lowest quartile, whether inside or outside of the halo.

Both due to the dispersal of satellite positions, and due to the changing satellite composition, satellite planes in the *host-centric* frame have short lifetimes. The only examples of satellite planes with lifetimes beyond 0.6 Gyr in the *host-centric* frame are those in which the composition of satellites has changed over time. By contrast, in the *satellite-centric* frame, several systems maintain planes for several Gyr. In all of these cases, the anisotropy has invariably been maintained outside of the host halo, and before some of the subhalos constituting the  $t = 0$  plane have become satellites.

##### 6. CONCLUSION

Simulations in the  $\Lambda$ CDM paradigm can produce highly anisotropic satellite systems, but their evolution and apparent lifetime is a matter of perspective. Within any given halo, planes of satellites are transient, identifiable for only a few hundred Myr. However, the progenitors of the present-day satellites may have maintained

persistent coherence for several Gyr, beyond the time that many of them have been satellites of the same halo.

Differences between previous studies also arise from applying different anisotropy metrics to different subsets of satellites in different simulations. For example, Santos-Santos et al. (2023) and Gámez-Marín et al. (2025) have pointed out that subsets of satellites with aligned orbital poles can exhibit persistent spatial anisotropies. However, our results suggest that the disagreement on whether spatial anisotropies are persistent or transient may be even more basic as a result of different reference frames. Studies that have found only short-lived features have largely considered the evolution of halos and their evolving satellite systems in the *host-centric* frame. By contrast, those studies that have found long-lived features have invariably adopted the *satellite-centric* frame, tracing the history of the satellite progenitors themselves, often beyond their infall times.

This understanding also reconciles the two apparently conflicting theoretical predictions: the anisotropic and correlated distributions of satellites before infall predicted by  $\Lambda$ CDM can lead to anisotropic satellite systems, which, when traced back in time, appear long-lived (e.g. Li & Helmi 2008; Libeskind et al. 2015; Gámez-Marín et al. 2024). However, this is not in conflict with the finding that, once within a halo, satellite planes must be short-lived (Fernando et al. 2017, 2018). The former considers anisotropies in the *satellite-centric* frame, while the latter considers the *host-centric* frame. The longevity of planes in the *satellite-centric* frame relies on the fact that satellites only spend a short time inside the halo, where any planes quickly dissolve.

The limited resolution of TNG-50 likely also affects the time evolution of satellite planes, but this is unlikely to be the main driver for the different behaviour between the two frames we describe here. Future, higher resolution simulations will be required to confirm this, and to extend our analysis to planes with genuine high anisotropies.

Our work cannot directly address the question of whether the actual Milky Way's plane of satellites is transient. Simple backwards orbital integration suggests that it disperses within a few hundred Myr of lookback time, even under idealised conditions (e.g. Maji et al. 2017; Sawala et al. 2023a), although Kumar et al. (2025) caution that this may underestimate the effect of observational errors. Perhaps more importantly, by integrating closed orbits of the present-day satellites in a static potential, these studies neither account for the past disruption of satellites, nor for the finite infall times of the present satellite population. Our results suggest that both of these effects could potentially shorten the lifetime of the MW's plane in a *host-centric* frame. A clear answer and a more meaningful comparison to simulation results may therefore not only require more precise observations of the present-day satellite system, but also accounting for the evolving potential.

We conclude that, as a prediction of the  $\Lambda$ CDM model, within a given galaxy, satellite planes represent only a brief phase, with lifetimes that rarely exceed a few hundred million years. However, these satellite planes are not all ephemeral, chance alignments: they can consist of substructures whose anisotropies can be traced back over several Gyr. Satellite planes that are transient in

the *host-centric* frame can be persistent in the *satellite-centric* frame.

#### CODE & DATA AVAILABILITY

Documented code to reproduce all results and figures presented in this paper is provided at:

[www.github.com/TillSawala/transient-persistent](https://www.github.com/TillSawala/transient-persistent).

Reduced data and variants of the plots for  $N = [9 \dots 13]$  satellites and for  $r_{\text{lim}} = r_{200}$  are included. The code can also easily be used to consider, for example, different numbers or subsets of satellites, different definitions of  $r_{\text{lim}}$ , of the lifetime,  $\tau$ , or different lookback time intervals. The underlying simulation data is available at:

[www.tng-project.org](http://www.tng-project.org).

#### ACKNOWLEDGEMENTS

I thank Isabel Santos-Santos, Jenni Häkkinen, Peter Johansson and Gabor Racz for very helpful comments. I thank the creators of the TNG-50 simulation for making their data public, and the Flatiron Institute and the Simons Foundation for travel support at the start of the project. I acknowledge support by Research Council of Finland grants 354905 and 339127, and ERC Consolidator Grant KETJU (no. 818930). This work used facilities hosted by the CSC—IT Centre for Science, Finland. I also gratefully acknowledge the use of open-source software, including `Matplotlib` (Hunter 2007), `SciPy` (Virtanen et al. 2020) and `NumPy` (Harris et al. 2020).

#### REFERENCES

Boylan-Kolchin M., 2021, *Nature Astronomy*, **5**, 1188  
 Buck T., Dutton A. A., Macciò A. V., 2016, *MNRAS*, **460**, 4348  
 Bullock J. S., Boylan-Kolchin M., 2017, *ARA&A*, **55**, 343  
 Davis M., Efstathiou G., Frenk C. S., White S. D. M., 1985, *ApJ*, **292**, 371  
 Fernando N., Arias V., Guglielmo M., Lewis G. F., Ibata R. A., Power C., 2017, *MNRAS*, **465**, 641  
 Fernando N., Arias V., Lewis G. F., Ibata R. A., Power C., 2018, *MNRAS*, **473**, 2212  
 Frenk C. S., White S. D. M., Davis M., Efstathiou G., 1988, *ApJ*, **327**, 507  
 Gámez-Marín M., Santos-Santos I., Domínguez-Tenreiro R., Pedrosa S. E., Tissera P. B., Gómez-Flechoso M. Á., Artal H., 2024, *ApJ*, **965**, 154  
 Gámez-Marín M., Domínguez-Tenreiro R., Santos-Santos I., Pedrosa S. E., 2025, arXiv e-prints, p. arXiv:2509.13622  
 Grand R. J. J., et al., 2021, *MNRAS*, **507**, 4953  
 Harris C. R., et al., 2020, *Nature*, **585**, 357  
 Hu C., Tang L., 2025, *ApJ*, **979**, 187  
 Hunt J. A. S., Vasiliev E., 2025, *New A Rev.*, **100**, 101721  
 Hunter J. D., 2007, *Computing in Science & Engineering*, **9**, 90  
 Ibata R. A., et al., 2013, *Nature*, **493**, 62  
 Ibata R. A., Ibata R. A., Famaey B., Lewis G. F., 2014, *Nature*, **511**, 563  
 Kroupa P., 2012, *PASA*, **29**, 395  
 Kroupa P., Theis C., Boily C. M., 2005, *A&A*, **431**, 517  
 Kumar P., Pawłowski M. S., Kanehisa K. J., Li P., Júlio M. P., Taibi S., 2025, *A&A*, **699**, A363  
 Li Y.-S., Helmi A., 2008, *MNRAS*, **385**, 1365  
 Libeskind N. I., Frenk C. S., Cole S., Helly J. C., Jenkins A., Navarro J. F., Power C., 2005, *MNRAS*, **363**, 146  
 Libeskind N. I., Hoffman Y., Tully R. B., Courtois H. M., Pomarède D., Gottlöber S., Steinmetz M., 2015, *MNRAS*, **452**, 1052  
 Lynden-Bell D., 1976, *MNRAS*, **174**, 695  
 Madhani J. P., et al., 2025, arXiv e-prints, p. arXiv:2504.18515  
 Maji M., Zhu Q., Marinacci F., Li Y., 2017, *ApJ*, **843**, 62  
 Müller O., Pawłowski M. S., Jerjen H., Lelli F., 2018, *Science*, **359**, 534  
 Müller O., et al., 2021, *A&A*, **645**, L5  
 Nelson D., et al., 2019a, *Computational Astrophysics and Cosmology*, **6**, 2  
 Nelson D., et al., 2019b, *MNRAS*, **490**, 3234  
 Pawłowski M. S., 2018, *Modern Physics Letters A*, **33**, 1830004  
 Pawłowski M. S., Kroupa P., 2020, *MNRAS*, **491**, 3042  
 Pawłowski M. S., Sohn S. T., 2021, *ApJ*, **923**, 42  
 Perivolaropoulos L., Skara F., 2021, arXiv e-prints, p. arXiv:2105.05208  
 Pillepich A., et al., 2019, *MNRAS*, **490**, 3196  
 Pillepich A., et al., 2024, *MNRAS*, **535**, 1721  
 Sales L. V., Wetzel A., Fattah A., 2022, *Nature Astronomy*, **6**, 897  
 Samuel J., Wetzel A., Chapman S., Tollerud E., Hopkins P. F., Boylan-Kolchin M., Bailin J., Faucher-Giguère C.-A., 2021, *Monthly Notices of the Royal Astronomical Society*, **504**, 1379–1397  
 Santos-Santos I., et al., 2020, *ApJ*, **897**, 71  
 Santos-Santos I., et al., 2023, *ApJ*, **942**, 78  
 Sawala T., et al., 2023a, *Nature Astronomy*, **7**, 481  
 Sawala T., Teerlaho M., Johansson P. H., 2023b, *MNRAS*, **521**, 4863  
 Seo C., Yoon S.-J., Paudel S., An S.-H., Moon J.-S., 2024, *ApJ*, **976**, 253  
 Shao S., Cautun M., Frenk C. S., 2019, *MNRAS*, **488**, 1166  
 Uzeirbegovic E., et al., 2024, *MNRAS*, **535**, 3775  
 Virtanen P., et al., 2020, *Nature Methods*, **17**, 261  
 Xu Y., Kang X., Libeskind N. I., 2023, *ApJ*, **954**, 128  
 Zhao X., Mathews G. J., Phillips L. A., Tang G., 2023, *Galaxies*, **11**, 114  
 van den Bosch F. C., Ogiya G., 2018, *MNRAS*, **475**, 4066

This paper was built using the Open Journal of Astrophysics L<sup>A</sup>T<sub>E</sub>X template. The OJA is a journal which provides fast and easy peer review for new papers in the `astro-ph` section of the arXiv, making the reviewing process simpler for authors and referees alike. Learn more at <http://astro.theoj.org>.